Sustained signalling from the insulin receptor after stimulation with insulin analogues exhibiting increased mitogenic potency

Bo Falck HANSEN*‡, Gillian M. DANIELSEN*, Kirsten DREJER*, Anders R. SØRENSEN*, Finn C. WIBERG*, Harald H. KLEIN† and Anker G. LUNDEMOSE*

*Health Care Discovery, Novo Nordisk A/S, Novo Alle, DK-2880 Bagsvaerd, Denmark, and †Department of Medicine, University of Lübeck, Lübeck, Germany

The metabolic and mitogenic potencies of six different insulin analogues were determined by measuring glucose transport in primary adipocytes and DNA synthesis in CHO cells respectively. Three analogues showed a disproportionately high mitogenic potency compared with their metabolic potency, and were up to 7 times more mitogenically than metabolically potent when compared with human insulin. The mitogenic/metabolic potency ratio of the analogues was found to be inversely correlated with the insulin receptor dissociation rate constant (K_d) in an exponential fashion ($r = 0.99$), with a disproportionately greater increase in mitogenic potential compared with metabolic potential for analogues with K_d values of less than 40 % of that of human insulin. To investigate the molecular mechanisms behind the correlation between the increased half-life of the receptor–ligand complex (low K_d) and mitogenicity, 3 h time-course experiments were performed. Slow ligand dissociation from the insulin receptor induced a parallel sustained activation of the insulin receptor tyrosine kinase. A similar pattern was observed for insulin receptor autophosphorylation and Shc phosphorylation, whereas the duration of insulin receptor substrate-1 phosphorylation with low-K_d analogues and with insulin was similar. Thus the increased half-life of the ligand–receptor complex induces sustained activation of the insulin receptor tyrosine kinase and sustained phoshorylation of Shc, which may be the cause of the disproportionately high mitogenic potency seen for some insulin analogues.

INTRODUCTION

The biological effects observed following insulin stimulation are pleiotropic and can generally be divided into two distinct categories: mitogenic responses and metabolic responses. Studies with anti-[insulin receptor (IR)] antibodies [1] and IR mutants [2–9] have indicated that signals leading to activation of the various biological responses can be separated at or near the level of the IR. Despite major advances within recent years it is not yet clear if the metabolic and mitogenic actions of insulin share a common mechanistic pathway or are the result of two or more diverging pathways emerging from the IR. Both metabolic and mitogenic signals are initiated by insulin binding to the IR at the cell surface, whereupon the receptor is autophosphorylated, followed by tyrosine phosphorylation of signalling molecules located immediately downstream. It has been shown that IR tyrosine kinase (IRTK) activity, and probably also phosphorylation of substrates, is necessary for most of the biological effects of insulin [10].

The principal downstream substrate for the IRTK is insulin receptor substrate-1 (IRS-1), which is a cytosolic protein containing at least 20 potential tyrosine phosphorylation sites [10]. Several of these phosphorylation sites have been shown to be phosphorylated *in vivo* [11], and subsequently interact with *src* homology 2 (SH2) domains of various signal transduction molecules, including phosphatidylinositol 3-kinase [12], SH2-domain-containing protein tyrosine phosphatase-2 (syp) [13], GRB2 [14] and Nck [15]. Thus IRS-1 may be viewed as a multisite 'docking protein', which after tyrosine phosphorylation activates various signalling pathways via interaction with SH2 domains [16]. Several other direct substrates for IRTK, including Shc, have been demonstrated [17–21]. Consequently, signals for the various biological effects of insulin could be separated at the level of substrate phosphorylation, either of different sites on IRS-1 or of different substrates. Alternatively, the timing (i.e. duration) and magnitude of the signal could be an important factor discriminating between different biological responses. This has been nicely demonstrated for extracellular signal-regulated kinase (ERK) activation, where sustained activation leads to differentiation of PC12 cells, whereas more transient activation induces cell proliferation [22,23].

Previous work has suggested that some insulin analogues demonstrate discrepancies between their ability to stimulate metabolic and mitogenic pathways ([24], and references therein). In particular, [B-Asp^{10}]insulin (where B-indicates the B-chain) was found to exhibit a 3.5-fold increase in binding affinity, a 2-fold increase in metabolic potency *in vitro* and a 10–20-fold increase in mitogenic potency [24]. It seems that there exists an inverse relationship between the mitogenic potency of insulin analogues and their receptor dissociation rate constant [24,25]. This indicates that, in parallel with ERK activation, the duration and magnitude of the insulin signal might be of importance for selection of biological responses. In the present study we have consequently examined the time course of activation after stimulation with insulin analogues with binding kinetics and/or biological properties that differ widely from those of insulin, in order to study the molecular mechanisms responsible for the increased mitogenic potency seen for some insulin analogues.

Abbreviations used: IR, insulin receptor; IRTK, insulin receptor tyrosine kinase; IRS-1, insulin receptor substrate-1; SH2, *src* homology 2; ERK, extracellular signal-regulated kinase; IGF-1, insulin-like growth factor-1; CHO, Chinese hamster ovary; CHO-hIR, CHO cells overexpressing the human insulin receptor; 3-O-MG, 3-*O*-methylglucose; DMEM, Dulbecco's modified Eagle's medium; PVDF, polyvinylidene difluoride.

‡ To whom correspondence should be addressed.

EXPERIMENTAL

Materials

Insulin analogues and human insulin were produced by recombinant DNA techniques and site-directed mutagenesis. Baker's yeast was used for the production, and the analogues were produced and purified as previously described [26,27]. The six analogues selected for this study were [B-Asp^{9},B-Glu^{27}]insulin (X2), [B-Asp^{28}]insulin (X14), [A-His^{8}]insulin (X8), [B-Asp^{10}]insulin (X10), [B-Glu^{10},B-des-Thr^{30}]insulin (X97) and [A-His^{8},B-His^{4},B-Glu^{10},B-His^{27}]insulin (H2) (where B- and A- indicate B- and A-chains respectively). Human insulin was used as the reference insulin. [^{125}I]Tyr^{A14}-labelled human insulin and analogues were prepared using the lactoperoxidase method as described by Drejer et al. [28]. [^{125}I]Tyr^{31}-labelled human insulin-like growth factor-1 (IGF-1) was prepared as described by Schäffer et al. [29].

Human serum albumin (dry purified) was obtained from Behringwerke (Marburg, Germany). Culture media, fetal calf serum, penicillin and streptomycin were from Gibco Life Technologies (Irvine, Scotland. U.K.). Tissue culture flasks and multiwell dishes were from Nunc (Roskilde, Denmark). Radiochemicals Na^{125}I, [*Me*-^{3}H]thymidine, 3-*O*-[^{3}H]methylglucose (3-O-[^{3}H]MG), ^{125}I-streptavidin and [^{32}P]ATP were obtained from Amersham (Aylesbury, Bucks., U.K.). Collagenase (CLS 1) was obtained from Worthington Biochemical Corp., and poly(Glu,Tyr) (4:1) was from Sigma. Other chemicals used were of analytical grade from Merck (Darmstadt, Germany).

Cell culture

Chinese hamster ovary (CHO) cells, K1 strain (A. T. T. C., Rockville, MD, U.S.A.), were cultured at 37 °C in a 5 % CO_2 humidified atmosphere in Nunclon culture flasks with nutrient mixture F-12 (Ham) medium supplemented with 10 % (v/v) fetal calf serum, 50 μg/ml streptomycin and 50 units/ml penicillin. Cells were subcultured at a 1:5 split ratio every 3–4 days for routine maintenance.

CHO cells overexpressing the human IR (CHO-hIR cells) were produced using the calcium phosphate-mediated transfection procedure [30] with subsequent glycerol shock [31]. The cDNA encoding the human IR lacking exon 11 was obtained as previously described [32]. At 2 days post-transfection, cells were trypsinized and diluted into selection medium containing 0.4–2.0 μM methotrexate. After 14 days, stable individual colonies were isolated using cloning rings and screened for expression of the IR by measuring the cell-surface binding of [^{125}I]Tyr^{A14}-labelled human insulin at 4 °C. Selected CHO-hIR clones were propagated for further studies. CHO-hIR cells were cultured at 37 °C in a 5 % CO_2 humidified atmosphere in Nunclon culture in Dulbecco's modified Eagle's medium (DMEM) supplemented with 10 % (v/v) fetal calf serum, 1 % non-essential amino acids, 50 μg/ml streptomycin, 50 units/ml penicillin and 1 μM methotrexate. Cells were subcultured at a 1:5 split ratio every 3–4 days for routine maintenance.

3-O-MG uptake

Primary rat adipocytes were prepared from epididymal fat-pads excised from 160–180 g Wistar rats (Møllgård Breeding Centre, Denmark) as previously described [33]. Briefly, finely minced tissue was shaken at 1 fat-pad per 2 ml of degradation buffer (0.4 mg/ml collagenase, 3 % BSA, 1.1 mM D-glucose, 10 mM Hepes, 2.5 mM $CaCl_2$, 4.7 mM KCl, 1.25 mM $MgSO_4$, 140 mM NaCl, 2.5 mM NaH_2PO_4, pH 7.4) in polypropylene vials, for 1 h at 37 °C, at 200 cycles/min. Cells were subsequently filtered through a nylon mesh (8.5P-160; Nytal; SS Thal) and washed with a Hepes/salt/albumin (HSA) buffer (140 mM NaCl, 2.5 mM $CaCl_2$, 4.7 mM KCl, 1.25 mM Mg_2SO_4, 2.5 mM NaH_2PO_4, 10 mM Hepes, 1 % albumin, pH 7.4), centrifuged at 200 ***g*** (Heraeus Megafuge 1.0R), and washed a further two times in HSA buffer. After the final wash, cells were resuspended to 40 % (v/v) cryocrit, and kept at 37 °C until used (within 2 h).

3-O-MG initial uptake was determined by a modification of the method described by Whitesell and Gliemann [33]. To determine the ED_{50}, 240 μl aliquots of cells at a packed cell volume of 40 % (v/v) were diluted to 4 % (w/v) in HSA buffer, and insulin or an insulin analogue added. For each ligand, eight or nine different doses were used. Adipocytes were incubated for 30 min at 37 °C, with resuspension at 5 min intervals. At the end of this period, cells were rapidly re-normalized to a packed cell volume of 40 % (v/v) by careful removal of infranatant and weighing of vials. Cells were immediately assayed by mixing 45 μl of adipocytes with 12 μl of 3-O-[^{3}H]MG (17 μCi/ml; 54 mCi/mmol), and the reaction stopped after 2 s by adding 3 ml of 0.3 mM phloretin in PBS at room temperature. After addition of 1 ml of silicone oil (DC 510/50; Bie & Berntsen), the polypropylene tube was centrifuged at 1200 ***g*** (Heraeus Megafuge 1.0R) for 1 min, and the adipocyte raft was removed with a short length of pipe cleaner. The samples were mixed well with 10 ml of Insta Gold Scintillant, and ^{3}H radioactivity was determined. Routinely, the equilibrium volume was determined by a 15 min uptake assay following maximal stimulation with insulin. All assays were run with quadruple samples. The data were analysed according to the four-parameter logistic model, and the metabolic potency of analogues was expressed relative to that of insulin [ED_{50}(insulin)/ED_{50}(analogue) × 100 %; $n = 2$].

Thymidine incorporation

CHO-K1 cells were seeded on 24-well Nunclon plates at a density of (1–3) × 10^4 cells/well and grown in serum-free F-12 (Ham) medium containing 5 μmol/l $FeSO_4$, 5 μg/ml transferrin, 20 ng/ml insulin, 7.5 mM Hepes, 2 mM glutamine, 2 mM pyruvate, 50 μg/ml streptomycin, 50 units/ml penicillin and 1 % non-essential amino acids (assay medium). After 3 days of culture the cells had reached half-confluence (approx. 2 × 10^5 cells/well), and insulin was then omitted from the above medium. After 24 h of quiescence the cells were incubated in assay medium containing increasing concentrations of insulin or insulin analogue and incubated for a further 18 h. For each ligand 12 different doses were used. [^{3}H]Thymidine (0.5 μCi/well) was subsequently added and the cells were incubated for 3 h. The reaction was stopped by 3 × 2 ml washes with ice-cold PBS. Cells were then solubilized in 0.4 % trypsin, DNA was isolated in a 12-channel Skatron Cell harvester, and incorporated ^{3}H was determined by β-radiation counting. The data were analysed according to the four-parameter logistic model and the mitogenic potency of analogues was expressed relative to that of insulin [ED_{50}(insulin)/ED_{50}(analogue) × 100 %; $n = 4$–5]. The mitogenic potency of each analogue was calculated by using the mean of the relative mitogenic potency from single assays, with a logarithmic scale and weighting according to the precision obtained in each assay.

Determination of dissociation rate constants

CHO-hIR cells were seeded on 24-well Nunclon plates at a density of 5 × 10^4 cells/well in DMEM containing 10 % fetal calf serum, 1 % non-essential amino acids, 20 mM Hepes, 1 g/l human albumin and 0.1 % bacitracin (pH 7.4); cells were used at

confluence. The kinetics of dissociation from CHO-hIR cells were analysed by incubating cells with 50 pM ^{125}I-labelled insulin or analogue for 3 h at 4 °C. Cells were washed quickly twice with ice-cold Hepes-buffered DMEM (pH 7.4) and the dissociation of radioactivity was measured after the addition of Hepes-buffered DMEM containing 0.1 μM unlabelled insulin in order to measure the maximal accelerated dissociation rate [34,35]. Cell-associated radioactivity was measured as a function of time, and the dissociation rate constants (K_d) were calculated using the LIGAND program [36].

Determination of receptor numbers

CHO-hIR and CHO-K1 cells were seeded on 24-well Nunclon plates at a density of 5×10^4 cells/well in DMEM containing 20 mM Hepes, 1 g/l human albumin, 10 % fetal calf serum, 1 % non-essential amino acids and 0.1 % bacitracin (pH 7.4); cells were used at confluence. The numbers of insulin and IGF-1 receptors present at the surface of the CHO-K1 and CHO-hIR cells were determined by saturation of the respective receptors with unlabelled ligand. Cells were incubated overnight at 4 °C with 50 pM ^{125}I-labelled insulin or [^{125}I]IGF-1 in the presence of increasing amounts of unlabelled insulin or IGF-1 respectively. The number of receptors was estimated with the aid of the LIGAND program fitting a two-site model [36]. The native CHO-K1 cells were estimated to express approx. 3000 high-affinity binding sites for insulin and 50000 IGF-1 receptors, whereas CHO-hIR cells were found to express 60000 IRs and 50000 IGF-1 receptors.

Time-course experiments

CHO-hIR cells were cultivated in DMEM containing 2 mM glutamine, 50 units/ml penicillin, 50 g/ml streptomycin, 10 % fetal calf serum, 1 % non-essential amino acids and 1 μM methotrexate. Cells were grown to 80 % confluence in 60 mm dishes, 6-well plates (IRTK activity assay) or 12-well plates before the experiments were carried out. Before stimulation with insulin or analogue, the cells were starved for 18 h in serum-free medium supplemented with 0.5 % insulin-free BSA. The cells were stimulated with 1 ml of 0.1 μM insulin or analogue for 30 min, then washed thoroughly 3–5 times (2–5 ml each wash) and subsequently incubated in serum- and insulin-free medium. Because of the large variations in receptor kinetics and potencies of the analogues, the high concentration of 0.1 μM and the 30 min stimulation time were used to ensure maximal stimulation. At various times post-stimulation (0–180 min) the medium was removed and the cells processed further as described below.

IRTK activity assay

IRTK activity was measured by a variation of the method described by Klein et al. [37]. In short, at the given time point post-stimulation, the incubation medium was removed and the cells immediately frozen by pouring liquid N_2 into the wells. A 400 μl aliquot of ice-cold solubilization buffer (20 mM Hepes, 8 mM EDTA, 0.2 mM Na_3VO_4, 10 mM $Na_4P_2O_7$, 2.5 mM PMSF, 1 mg/ml aprotinin, 2.5 mg/ml benzamidine, 2.5 μg/ml pepstatin, 2.5 μg/ml leupeptin, 160 mM NaF, 2 mM dichloroacetic acid, 1 % Triton X-100, pH 7.4) was added to each well and samples were transferred to a Potter–Elvehjem homogenizer and homogenized on ice. After 20 min at 4 °C, the samples were centrifuged at 20000 ***g*** for 60 min at 4 °C to remove cell debris. Microtitre wells were coated with an anti-IR antibody (Ab-3; Oncogene Science; 10 μg/ml) as described [37] and 30 μl of supernatant was added to each well. Insulin (final concentration 8.65 nM) was then added to all samples and, after incubation for 16 h at 4 °C, the supernatants were removed and the wells washed five times with wash buffer (0.05 % Triton X-100, 100 mM NaCl, 2.5 mM KCl, 1 mM $CaCl_2$, 0.1 mM Na_3VO_4, 20 mM Hepes, 10 % glycerol, 0.05 % NaN_3 and 0.5 % BSA, pH 7.4). The phosphorylation reaction was initiated by adding 25 μl of a mixture containing 0.05 % Triton X-100, 60 mM NaCl, 1.5 mM KCl, 0.6 mM $CaCl_2$, 0.06 mM Na_3VO_4, 12 mM Hepes, 5 mM $MnCl_2$, 12 mM $MgCl_2$, 500 μM CTP, 0.5 μM [^{32}P]ATP (3000 Ci/mmol) and 2 mg/ml poly(Glu,Tyr) (4:1), pH 7.4. The reaction was stopped after 20 min at 4 °C by adding 40 μl of ice-cold 100 mM ATP (pH 7.4). The contents of the wells were then spotted on to Whatman 3MM filter paper (1.5 cm × 1.5 cm); the filters were washed five times with ice-cold 10 % (w/v) trichloroacetic acid supplemented with 10 mM Na_2HPO_4 (10 ml/filter). The amount of P_i incorporated into poly(Glu,Tyr) (4:1) was quantified by PhosphorImager (Molecular Dynamics) analysis after 4–24 h exposure. The binding activity in each well was measured as described [37], except that ^{125}I-labelled analogue H2 was used instead of [^{125}I]insulin.

Tyrosine phosphorylation of IR, IRS-1 and Shc

At the given time points post-stimulation, the incubation medium was removed; cells were immediately frozen by pouring liquid N_2 into the wells and solubilized at 0 °C for 20 min in the following buffer: 50 mM Hepes, 10 mM EDTA, 1 mg/ml aprotinin, 2 mM PMSF, 2 mM Na_3VO_4, 100 mM NaF, 10 mM $Na_4P_2O_7$ and 1 % Nonidet P-40, pH 7.4. For immunoprecipitation, cell lysate samples were incubated with antibodies against the IR (Ab-3; Oncogene Science; 10 μg/ml), IRS-1 (polyclonal rabbit anti-IRS-1; UBI; 1.5 μg/ml) or Shc (rabbit polyclonal anti-Shc; Transduction Laboratories; 5 μg/ml) and kept on ice overnight. Antigen–antibody complexes were adsorbed on to Protein G–Sepharose or Protein A–Sepharose beads for 1 h at 4 °C during gentle agitation, before being collected by microcentrifugation at 20000 ***g*** at 4 °C for 10 s. Beads were washed three times in 50 mM Hepes, pH 7.4, 100 mM NaCl, 10 mM EDTA, 2 mM Na_3VO_4, 100 mM NaF, 10 mM $Na_4P_2O_7$ and 1 % Nonidet P-40 before solubilization in SDS sample buffer. Samples were separated by SDS/PAGE (6 % or 10 % gels), followed by transfer to polyvinylidene difluoride (PVDF) membranes (Immobilon; Millipore). Equal amounts of immunoprecipitated protein were loaded on to SDS/PAGE gels, as determined by Western blotting using anti-IR, anti-IRS-1 or anti-Shc antibodies. The PVDF membranes were blocked in 20 mM Tris (pH 7.5), 150 mM NaCl (TBS) with 3 % gelatin for 1 h at room temperature and reacted with primary antibody against phosphotyrosine (4G10; UBI; 1 μg/ml) in TBS/0.05 % Tween-20 for 2 h at room temperature. After three washes in TBS/0.05 % Tween-20, the membranes were incubated for 1 h at room temperature with polyclonal anti-(rabbit IgG) or anti-(mouse IgG) conjugated with biotin. Phosphorylated IR, IRS-1 or Shc proteins were visualized by ^{125}I-streptavidin. Band intensity was quantified by PhosphorImager analysis after 4–24 h screen exposure.

RESULTS AND DISCUSSION

Glucose transport

The metabolic potency of the various insulin analogues was determined by measuring dose–response relationships for the initial velocity of uptake of 3-O-MG, a non-metabolizable glucose analogue, following a 30 min stimulation period. Normally only a few minutes of insulin stimulation is required for full activation of glucose transport [38]. However, several of the analogues

Table 1 Relative biological potencies and relative dissociation rate constants for the selected insulin analogues

Biological potencies are expressed as ED_{50} values relative to that of insulin (means ± S.E.M.). The dissociation rate constants were calculated from dissociation curves using the LIGAND program and expressed relative to the K_d value for insulin (5.52×10^{-2} s^{-1}). For comparison, previously determined metabolic potencies, assessed by the lipogenesis assay, are included.

Analogue	Substitution	Relative ED_{50} (%)			Relative K_d (%)
		Glucose transport	Lipogenesis	Mitogenicity	
Insulin	–	100	100	100	100
X2	[B-Asp^{9},B-Glu^{27}]insulin	44 ± 1	31 ± 0.1	56 ± 7	139 ± 10
X14	[B-Asp^{28}]insulin	105 ± 13	101 ± 2	94 ± 11	81 ± 8
X8	[A-His^{8}]insulin	244 ± 14	309 ± 24	275 ± 47	39 ± 6
X10	[B-Asp^{10}]insulin	227 ± 21	207 ± 14	663 ± 77	14 ± 1
X97	[B-Glu^{10},B-des-Thr^{30}]insulin	254 ± 5	402 ± 35	541 ± 98	24 ± 4
H2	[A-His^{8},B-His^{4},B-Glu^{10},B-His^{27}]insulin	433 ± 50	572 ± 49	2954 ± 313	1.5 ± 0.1

exhibit slow binding kinetics [24], and a 30 min stimulation period was therefore applied to ensure full steady-state binding prior to metabolic testing. To avoid possible dose shifts due to insulin degradation, adipocytes were diluted during the stimulation period and reconcentrated to 40 % (v/v) cryocrit immediately prior to assay. There was no significant difference in absolute minimal (no ligand) or maximal (0.1 μM ligand) responses or in the slope of the dose–response curves for the analogues and for insulin (on average a 6.1 ± 0.3-fold stimulation was observed upon maximal stimulation). Consequently the metabolic potency of each analogue was expressed as its ED_{50} value as a percentage of that of insulin ($ED_{50} = 1.03 \times 10^{-10}$ M; Table 1). The metabolic potencies ranged from 44 % (X2) to 433 % (H2). For comparison, previously determined metabolic potencies [26], assessed by lipogenesis over a 2 h period and ranging from 31 to 572 %, are included in Table 1, and correlate well with the measurement of 3-O-MG uptake.

Thymidine incorporation

The mitogenic potency of the insulin analogues was determined by measuring dose–response relationships for [^{3}H]thymidine incorporation into DNA in CHO-K1 cells following an 18 h stimulation period. As for glucose transport, there was no significant difference in absolute minimal (no ligand) or maximal (0.1 μM) responses or in the slope of the dose–response curves for the analogues and for insulin (on average a 5.6 ± 0.3-fold increase was observed upon maximal stimulation). Consequently, the mitogenic potency for insulin analogues is expressed as the ED_{50} value relative to that of insulin ($ED_{50} = 2 \times 10^{-9}$ M). The mitogenic potencies had a much broader diversity than the metabolic potencies, ranging from 56 % (X2) to 2954 % (H2) (Table 1).

Dissociation rate constants

Dissociation rate constants (K_d) were measured as the dissociation of ^{125}I-labelled insulin or analogue from CHO cells overexpressing the human IR over a period of 3 h in the presence of unlabelled insulin or analogue. The experiments were carried out at 4 °C to minimize internalization, and results are expressed as a percentage of initial binding (Figure 1). H2 dissociated very slowly from the receptor (Figure 1, lower panel), whereas X2 dissociated more rapidly than insulin (Figure 1, upper panel). Thus approx. 90 % of the initial binding was still present after 3 h for H2, but under 5 % remained for X2, compared with approx. 11 % for insulin. In fact, one-third of the initial bound H2 was

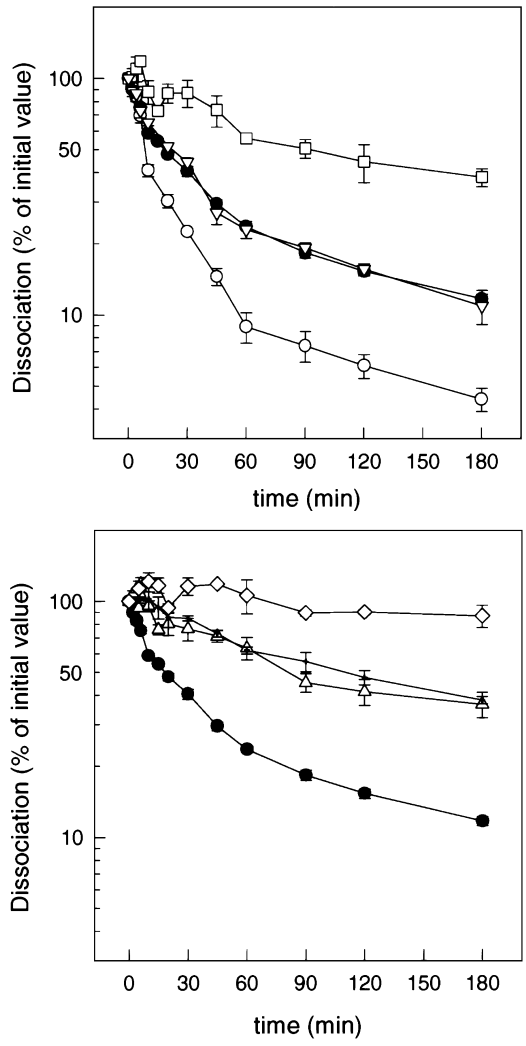

Figure 1 Kinetics of dissociation of insulin and analogues from CHO-hIR cells

Dissociation was analysed by incubating CHO-hIR cells with ^{125}I-labelled insulin or analogue for 3 h at 4 °C. Cells were then washed quickly twice and dissociation determined after the addition of 0.1 μM unlabelled insulin or analogue. Cell-associated radioactivity was measured as a function of time and residual binding expressed as a percentage of initial binding. Top: ●, insulin; ▽, X14; ○, X2; □, X10. Bottom: ●, insulin; ◇, H2; △, X8; +, X97. Values are means ± S.E.M. ($n = 4$).

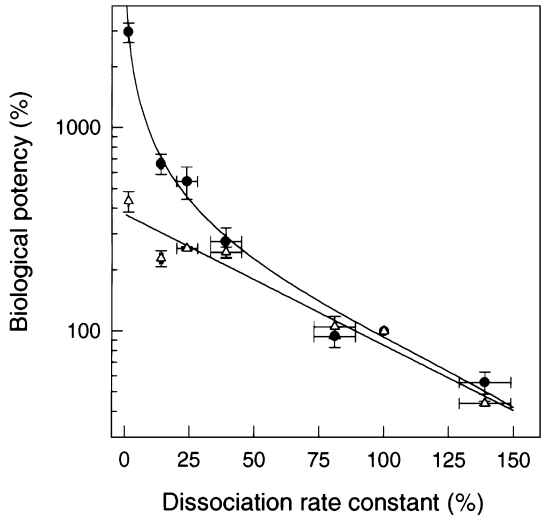

Figure 2 Relationship between dissociation rate constants and biological potencies

Initial dissociation rate constants (K_d), expressed as a percentage of that of insulin, were calculated from the data in Figure 1 and plotted against mitogenic and metabolic potencies (ED_{50} values as a percentage of that of insulin, measured as described in the Experimental section). ●, Mitogenic potency; ○, metabolic potency (3-O-MG uptake). Values are presented as means ± S.E.M. For biological potencies the relationship was best described by an exponential function {metabolic potency $= \exp[2.54-(6.43\times10^{-3}K_d)]$; $r^2 = 0.95$}, whereas for mitogenic potencies the relationship was best described by a logistic function {mitogenic potency $= -100.2+7445/[1+(K_d/0.94)^{0.78}]$; $r^2 = 0.99$}.

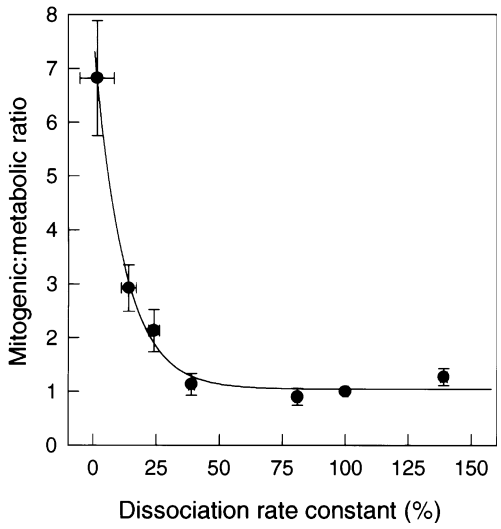

Figure 3 Correlation between K_d and the mitogenic/metabolic potency ratio

The relative dissociation rate constants (K_d) and relative biological potencies were calculated as described in the legend to Figure 2. Values are presented as means ± S.E.M. The relationship was best described by a exponential function [mitogenic/metabolic potency ratio $= 1.04+6.54\times\exp(-K_d/11.79)$; $r^2 = 0.99$].

found still to be bound after 24 h of incubation. Analogue X14 showed a time-dependent dissociation pattern very similar to that of insulin (Figure 1). Relative dissociation rates (K_d) fitted to a two-compartment model; the initial dissociation rate constants were estimated and ranged from 1.5% (H2) to 139% (X2) compared with insulin (100%) (Table 1).

Discrepant increases in mitogenicity for low-K_d analogues

In earlier studies of the insulin analogues, it was speculated that the increased mitogenicity of certain insulin analogues is related to a low receptor off-rate, with an inverse relationship between the dissociation rate constant and the mitogenic potency [24,25]. In the present study, an inverse relationship between the K_d and the mitogenic potency was indeed observed (Figure 2). However, a strong correlation between K_d and metabolic potency was also observed (Figure 2) and, furthermore, a strong correlation between receptor affinity and both metabolic and mitogenic potencies was also evident. Thus both high receptor affinity and low K_d correspond to high metabolic and mitogenic potency. It is clear, however, that the divergence between metabolic and mitogenic potencies increased with decreasing K_d, and when the mitogenic/metabolic potency ratio was plotted against K_d (Figure 3), a strong inverse exponential correlation was found ($r^2 = 0.99$). Thus, for insulin analogues with K_d values lower than approx. 40% of that of insulin, the ability to stimulate mitogenicity is increased in excess (up to 7-fold) of the ability to stimulate metabolism (Figure 3).

The relative K_d values of the insulin analogues were determined by measuring dissociation from the cell surface at neutral pH, under conditions minimalizing internalization (4 °C), and the values thus represent ranking of the dissociation of ligand from receptor at the cell surface prior to internalization. However, under normal culture conditions, cessation of ligand signalling after internalization is undoubtedly of greater biological significance, with an increase in dissociation as the ligand–receptor complex is internalized into the acidic endosomal compartment. During this process a gradual transit down a pH gradient from the extracelluar pH (7.4) to approx. pH 5 occurs. For insulin and the most intensively studied of the representative low-K_d analogues, X10, dissociation from the purified human IR was evaluated as a function of pH (values of 7.0, 6.2, 5.4, 4.6) at 20 °C. When dissociation was expressed as the $t_{\frac{1}{2}}$ for ligand release normalized to initial ligand bound, corrected for non-specific binding, the same relative dissociation was observed, with a slight relative increase (10%) in the $t_{\frac{1}{2}}$ for X10 at pH 5.4. Relative dissociation at pH values lower than 5.4 is unreliable, due to the rapid dissociation of human insulin (G. M. Danielsen, unpublished work). Thus, for X10 at least, the relative dissociation is maintained down the physiological pH gradient.

Role of the IGF-1 receptor in mitogenicity

In order to exclude the possibility of a discrepantly large increase in IGF-1 receptor affinity compared with IR affinity for the insulin analogues, the relative affinities for both receptors were determined. Like human insulin, the analogues included in this study had an IR affinity that paralleled the IGF-1 receptor affinity, with an approximate 1000-fold lower affinity for the IGF-1 receptor compared with the IR. However, we cannot exclude the possibility that insulin analogues may exhibit part of their mitogenic effect through the IGF-1 receptor, even though it seems to be mediated primarily through the IR. The latter is based on the observation that insulin analogues exhibit the same ranking and order of mitogenic potency in LB cells, a cell line lacking IGF-1 receptors (B. Ursø, personal communication; [25]).

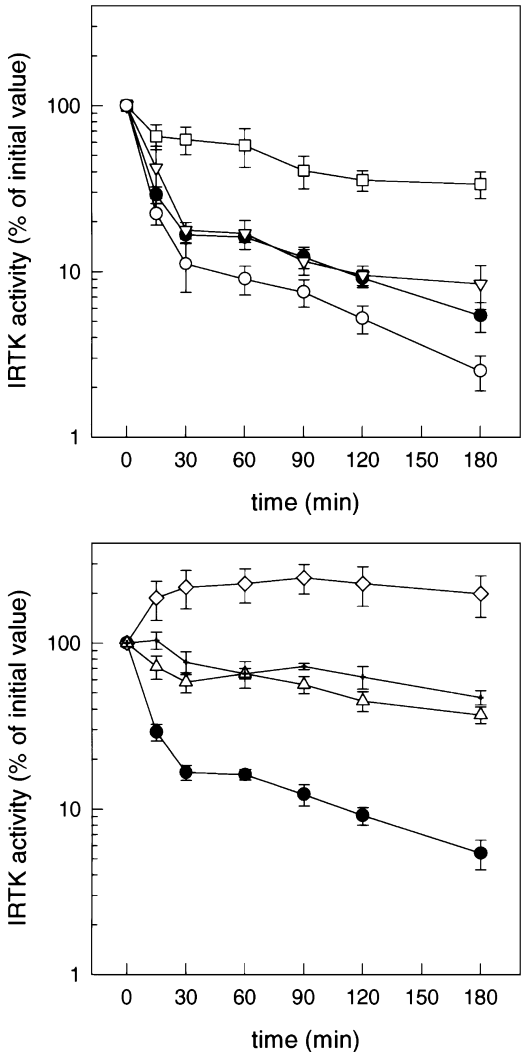

Figure 4 Time course of IRTK activation

CHO-hIR cells were serum-starved for 18 h and subsequently stimulated with 0.1 μM insulin or analogues for 30 min, then washed thoroughly to remove unbound ligand. At the indicated time points following stimulation, cells were immediately frozen and homogenized on ice. IRTK activity was then determined as described in the Experimental section. Values are expressed as a percentage of the initial value. Top: ●, insulin; ▽, X14; ○, X2; □, X10. Bottom: ●, insulin; ◇, H2; △, X8; +, X97. Values are mean ± S.E.M.; $n = 8$ for insulin and $n = 4$ for insulin analogues.

Time course of activation/phosphorylation of signalling elements

To examine whether the increased half-life of the ligand–receptor complex (low K_d) observed for several insulin analogues (Figure 1) resulted in parallel sustained receptor activation, the duration of IRTK activity and of IR, IRS-1 and Shc tyrosine phosphorylation was determined following a pulse stimulation by insulin or analogue. IRTK activity was determined in a microtitre well assay as phosphorylation of the synthetic substrate poly(Glu,Tyr) (4:1) [37]. Tyrosine phosphorylation of IR itself, as well as of IRS-1 and Shc, was measured by immunoprecipitation followed by anti-phosphotyrosine Western blotting and PhosphoImager detection. IRTK activity, IR autophosphorylation, IRS-1 phosphorylation and Shc phosphorylation were assessed at 0, 15, 30, 60, 90 (IRTK only), 120 and 180 min post-stimulation. Time-course studies with the IRTK activity assay revealed that at least a 30 min stimulation period was necessary to ensure steady-state activation for insulin analogues with slow binding kinetics.

Insulin receptor tyrosine kinase activity

The decline in IRTK activity following insulin/analogue stimulation and subsequent removal is shown in Figure 4. For insulin, a rapid decline in IRTK activity down to ~ 15% of the initial value was observed during the first 30 min post-stimulation. From 30 to 180 min post-stimulation a relatively slower decline in IRTK activity was observed. At 180 min the IRTK activity was only 5% of the initial value, but was still significantly elevated compared with unstimulated values (results not shown).

The analogue that displayed the fastest receptor dissociation, X2, was observed to display a more rapid decline in IRTK activity than insulin (Figure 4, upper panel). The decline in IRTK activity after stimulation with X14 again showed a pattern almost identical to that of insulin, whereas the low-K_d analogues X10, X8 and X97 showed a slower decline (Figure 4). For the high-affinity analogue H2, however, the IRTK activity was actually found to increase with time during the first 90 min post-stimulation (to 2.5 times the initial value), whereafter a small decline in IRTK activity was seen. Thus the decline in IRTK activity exhibited a strikingly similar pattern to ligand dissociation from the receptor, with the exception of analogue H2, showing that sustained activation of the IRTK directly paralleled the prolonged half-life of the ligand–receptor complex.

The paradoxical increase in IRTK activity observed with H2 is consistent with the recently proposed model for insulin binding to the IR [39]. This model predicts that each of the two subunits of the IR possesses two discrete ligand binding sites corresponding to two binding regions on the insulin molecule. If it is assumed that binding of two ligand molecules (at high ligand concentrations) inhibits IRTK activity, the increase in IRTK activity observed after H2 stimulation could result from a gradual decrease in ligand binding with time. In fact, dose–response studies with H2 revealed that IRTK activity decreases to approx. 40% of the maximal response at 0.1 μM ligand. All other insulin analogues used in this study had higher ED_{50} values than H2, and did not show the same phenomenon at the concentrations used for this series of experiments.

IR, IRS-1 and Shc phosphorylation

Although the IRTK activity measured in this study reflects *in vivo* activity, differences between IRTK activity and phosphorylation of endogenous substrates can be envisaged. Therefore three representative analogues were selected for tyrosine phosphorylation time-course studies: X2 (high K_d), X10 and H2 (both low K_d). IR autophosphorylation diminished in a time-dependent manner following withdrawal of insulin (Figure 5, top). The pattern of the decline in IR autophosphorylation after stimulation with insulin was similar to the pattern observed for IRTK activity, i.e. a rapid decrease during the first 30 min post-stimulation, followed by a slower decline during the next 30–180 min (Figure 6, top). For the high-K_d analogue X2 the tyrosine phosphorylation was much less protracted, with the signal almost abolished by 15 min post-stimulation. In contrast, the analogues with low K_d (H2 and X10) showed sustained phosphorylation of the IR throughout the period examined as compared with insulin. For H2 a time-dependent increase in phosphorylation was seen, parallel to the effect seen on IRTK activity. Thus the patterns of IRTK and IR autophosphorylation were in all cases very similar.

A similar pattern was observed for Shc phosphorylation (Figures 5 and 6, bottom panels): phosphorylation rapidly

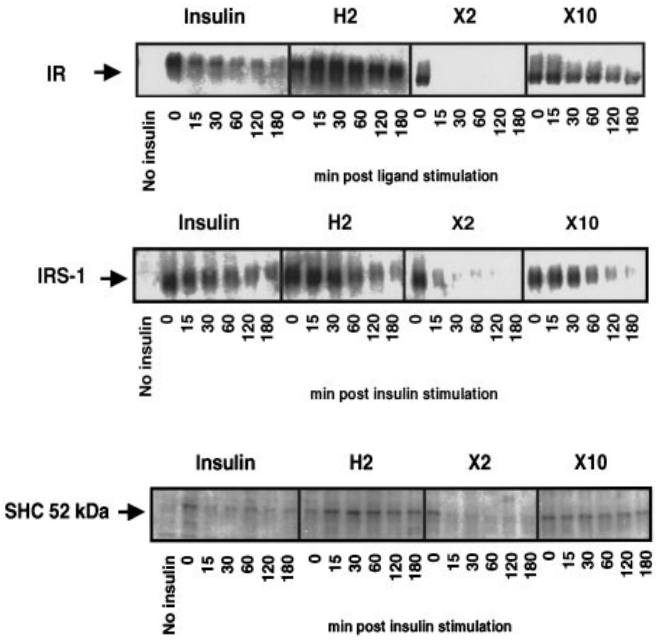

Figure 5 Tyrosine phosphorylation of the IR, IRS-1 and Shc

CHO-hIR cells were serum-starved for 18 h and subsequently stimulated with 0.1 μM insulin or analogues for 30 min, then washed thoroughly to remove unbound ligand. At the indicated times post-stimulation, the incubation medium was removed and cells immediately frozen. For immunoprecipitation, cell lysate samples were incubated with antibodies against the IR, IRS-1 or Shc. Antigen–antibody complexes were adsorbed on to Protein G–Sepharose or Protein A–Sepharose beads and the beads were washed and solubilized in SDS sample buffer. Samples containing equal amounts of immunoprecipitated protein were separated by SDS/PAGE followed by transfer to PVDF membranes, and incubated first with primary antibody against phosphotyrosine, then with biotin-conjugated polyclonal anti-(rabbit IgG) or anti-(mouse IgG). Phosphorylated IR, IRS-1 or Shc protein was visualized by ^{125}I-streptavidin. Band intensities were visualized by PhosphorImager analysis. Top, autophosphorylation of the IR; middle, IRS-1 phosphorylation; bottom, Shc phosphorylation.

decreased after removal of insulin, and the analogues H2 and X10 caused sustained Shc phosphorylation compared with insulin. Again a time-dependent increase in phosphorylation following ligand removal occurred after stimulation with analogue H2. The phosphorylation of Shc after stimulation with the high-K_d analogue X2 did not decrease more quickly than after stimulation with insulin, but this might be explained by the low number of counts in the bands after 30 min for X2.

In contrast to the the similar patterns observed for IRTK activity, IR autophosphorylation and Shc phosphorylation, the pattern for IRS-1 phosphorylation was different in that the rates of decrease in phosphorylation after stimulation with H2 and X10 were no different from the rate of decrease after stimulation with insulin (Figures 5 and 6, middle panels). Thus the increased half-life of the receptor–ligand complex results in prolonged IRTK activation, IR phosphorylation and Shc phosphorylation, but not prolonged IRS-1 phosphorylation.

Effect of low K_d in mitogenic signalling

The observed relationship between the prolonged half-life of the ligand–receptor complex and increased mitogenic potency could be due to an interplay of several effects of prolonged IRTK activity. These effects can be broadly classified as follows: (a) alteration in the pattern and/or magnitude of tyrosine phosphorylation of early signalling elements; (b) a temporal effect, i.e.

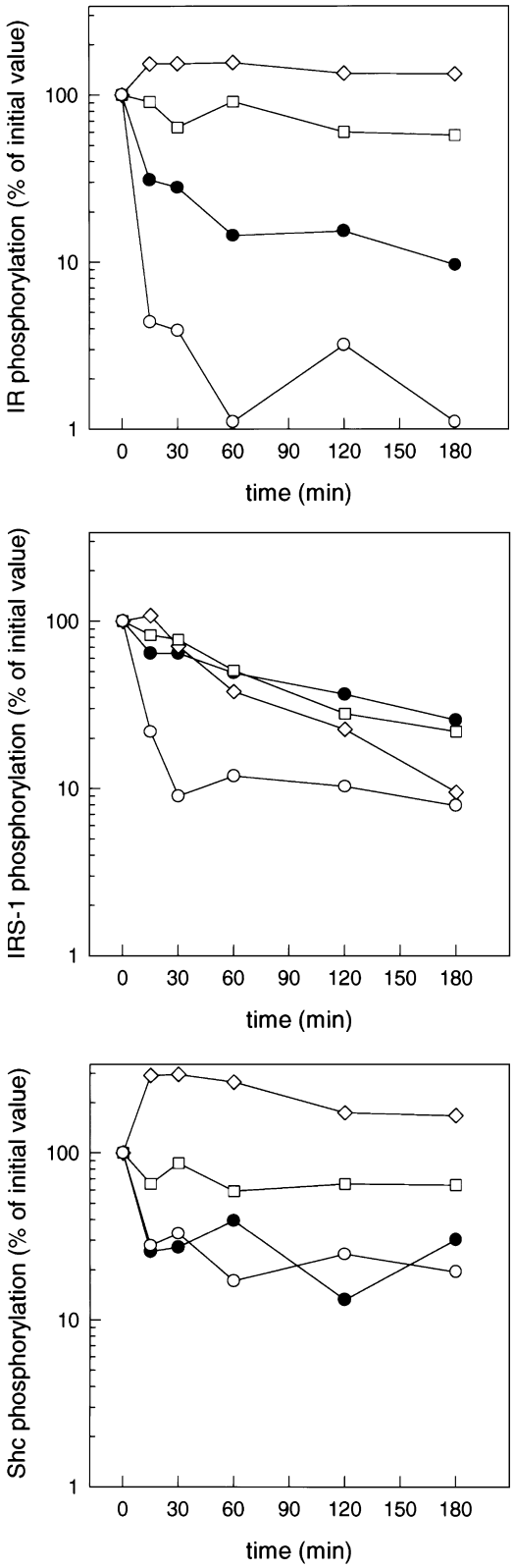

Figure 6 Quantification of tyrosine phosphorylation of the IR, IRS-1 and Shc

Bands on membranes shown in Figure 5 were quantified by PhosphorImager analysis after screen exposure for 4–24 h. Top, autophosphorylation of the IR; middle, IRS-1 phosphorylation; bottom, Shc phosphorylation. Symbols: ●, insulin; ○, X2; □, X10; ◇, H2.

sustained activation of signalling elements; and (c) a spatial effect, i.e. a shift in the intracellular locus of active signalling molecules. The following speculation contains elements from all these possibilities.

Increased mitogenicity could result from an altered phosphorylation pattern of the IR or substrates. Thus sustained activation of the IRTK could favour phosphorylation fingerprinting that is balanced towards mitogenic signalling, giving rise to interactions with and/or phosphorylation of cytosolic signalling molecules that are otherwise not encountered. With regard to the degree of phosphorylation at individual sites, the present analysis cannot discriminate between individual sites for the IR and IRS-1.

Since IRTK activity, IR autophosphorylation and Shc phosphorylation, but not IRS-1 phosphorylation, were sustained after stimulation with H2 and X10, this indicates a greater importance of Shc than of IRS-1 for mitogenic signalling by insulin. In accordance with this, Sasaoka et al. [40,41] found that microinjection of anti-Shc antibodies inhibited insulin-stimulated DNA synthesis in Rat1 fibroblasts, and that Shc played a more important role in insulin-stimulated $p21^{ras}$-GTP formation than did IRS-1. Thus it is possible that IRS-1 mainly mediates the metabolic effects of insulin, while Shc is responsible for the majority of the mitogenic effects.

The difference in the dephosphorylation patterns with the IR and Shc versus that with IRS-1 indicates that protein tyrosine phosphatases ensure a time-dependent dephosphorylation of IRS-1 despite ongoing activity of the IRTK, and that these phosphatases do not dephosphorylate the IR or Shc to a similar degree. Therefore the increased mitogenic signal may simply be related to sustained signalling from the IR. In this respect it is interesting that the secretion pattern of IGF-1, which is regarded to be of greater importance for growth than insulin, is more continuous than that of insulin. In addition, it is well known that several hours of stimulation are necessary to elicit a mitogenic response. Furthermore, the intracellular itineraries of IGF-1 and insulin and their respective receptors differ in several ways [42]. IGF-1 is preferentially targeted to the retroendocytotic pathway, wheras insulin primarily undergoes lysosomal degradation [42]. Thus the low-K_d insulin analogues, allowing for the possibility of the presence of sustained ligand–receptor complexes at intracellular locations, may induce a more IGF-1-like response through the IR than the more rapidly dissociating ligands, including insulin. In liver parenchymal cells, where insulin is largely related to metabolic effects and epidermal growth factor to mitogenic effects, it has been suggested that regulation of this specificity occurs at the level of the endosome, with rapid dissociation/degradation of insulin in the endosome limiting the time frame of IR activation and playing an important role in signalling specificity [43]. Furthermore, recent work supports the concept that the duration and magnitude of the signal are critical for the selection of biological responses [44,45].

In summary, we have demonstrated a close inverse relationship between the dissociation rate constant and the mitogenic/metabolic potency ratio of insulin analogues. The prolonged half-life of the ligand–receptor complex observed for some insulin analogues results in sustained activation of the IRTK and phosphorylation of Shc, but not of IRS-1. This may be the cause of the increased mitogenic/metabolic potency ratio of these insulin analogues. Thus the mitogenic response to insulin may be correlated with the duration of stimulation and be dependent upon Shc phosphorylation. This might explain why different receptors showing tyrosine kinase activity, although using the same substrates (e.g. insulin and IGF-1 receptors), result in different cellular responses.

We are indebted to Marianne Heiden, Pia Jensen, Anette Garval, Birgitte Skjølstrup, Maren Drenckhan, Bente Hansen and Jytte Topp Radzikowska for expert technical assistance, Ulla Dahl Larsen for providing radiolabelled insulin and insulin analogues, and Lauge Schäffer, Steen Gammeltoft and Pierre De Meyts for fruitful discussions.

REFERENCES

1 Ponzio, G., Contreres, J.-O., Debant, A., Baron, V., Gautier, N., Dolais-Kitabgi, J. and Rossi, B. (1988) EMBO J. **7**, 4111–4117
2 Takata, Y., Webster, N. J. G. and Olefsky, J. M. (1992) J. Biol. Chem. **267**, 9065–9070
3 Wilden, P. A., Siddle, K., Haring, E., Backer, J. M., White, M. F. and Kahn, C. R. (1992) J. Biol. Chem. **267**, 13719–13727
4 Rolband, G. C., Williams, J. F. and Olefsky, J. M. (1993) Endocrinology (Baltimore) **133**, 1437–1443
5 Wilden, P. A., Backer, J. M., Kahn, C. R., Cahill, D. A., Schroeder, G. J. and White, M. F. (1990) Proc. Natl. Acad. Sci. U.S.A. **87**, 3358–3362
6 Takata, Y., Webster, N. J. G. and Olefsky, J. M. (1991) J. Biol. Chem. **266**, 9135–9139
7 Thies, R. S., Ullrich, A. and McClain, D. A. (1989) J. Biol. Chem. **264**, 12820–12825
8 Debant, A., Clauser, E., Ponzio, G., Filloux, C., Auzan, C., Contreres, J.-O. and Rossi, B. (1988) Proc. Natl. Acad. Sci. U.S.A. **85**, 8032–8036
9 Pang, L., Milarski, K. L., Ohmichi, M., Takata, Y. and Saltiel, A. R. (1994) J. Biol. Chem. **269**, 10604–10608
10 White, M. F. and Kahn, C. R. (1994) J. Biol. Chem. **269**, 1–4
11 Sun, X. J., Crimmins, D. L., Myers, M. G. and White, M. F. (1993) Mol. Cell. Biol. **13**, 7418–7428
12 Backer, J. M., Myers, M. G., Jr., Shoelson, S. E., Chin, D. J., Sun, X. J., Miralpeix, M., Hu, P., Margolis, B., Skolnik, E. Y., Schlessinger, J. and White, M. F. (1992) EMBO J. **11**, 3469–3479
13 Kuhne, M. R., Pawson, T. and Feng, G. S. (1993) J. Biol. Chem. **268**, 11479–11481
14 Skolnik, E. Y., Batzer, A., Li, N., Lee, C. H., Lowenstein, E., Mohammadi, M., Margolis, B. and Schlessinger, J. (1993) Science **260**, 1953–1955
15 Lee, C. H., Li, W., Nishimura, R., Zhou, M., Batzer, A. G., Myers, M. G., White, M. F. and Skolnik, E. Y. (1993) Proc. Natl. Acad. Sci. U.S.A. **90**, 11713–11717
16 Sun, X. J., Rothenberg, P., Kahn, C. R., Backer, J. M., Araki, E., Wilden, P. A., Cahill, D. A., Goldstein, B. J. and White, M. F. (1991) Nature (London) **352**, 73–77
17 Pronk, G. J., McGlade, J., Pelicci, G. and Bos, J. L. (1993) J. Biol. Chem. **268**, 5748–5753
18 Sadoul, J., Peyron, J., Ballotti, R., Debant, A., Fehlmann, M. and Van Obberghen, E. (1985) Biochem. J. **227**, 887–892
19 Miralpeix, M., Sun, X. J., Backer, J. M., Myers, M. G., Araki, E. and White, M. F. (1992) Biochemistry **31**, 9031–9039
20 Uchida, T., Matozaki, T., Noguchi, T., Yamao, T., Horita, K., Suzuki, T., Fujioka, Y. and Kasuga, M. (1994) J. Biol. Chem. **269**, 12220–12228
21 Hosomi, Y., Shii, K., Ogawa, W., Matsuba, H., Yoshida, M., Okada, Y., Yokono, K., Kasuga, M. and Roth, R. A. (1994) J. Biol. Chem. **269**, 11498–11502
22 Traverse, S., Seedorf, K., Paterson, H., Marshall, C. J., Cohen, P. and Ullrich, A. (1994) Curr. Biol. **4**, 694–701
23 Dikic, I., Schlessinger, J. and Lax, I. (1994) Curr. Biol. **4**, 702–708
24 Drejer, K. (1992) Diabetes-Metab. Rev. **8**, 259–286
25 De Meyts, P., Christoffersen, C. T., Ursø, B., Ish-Shalom, D., Sacerdoti-Sierra, N., Drejer, K., Schäffer, L., Shymko, R. M. and Naor, D. (1993) Exp. Clin. Endocrinol. **101**, 22–23
26 Brange, J., Owens, D. R., Kang, S. and Vølund, A. (1990) Diabetes Care **13**, 923–954
27 Markussen, J., Diers, I., Langkjaer, L., Norris, K., Snel, L., Sørensen, A. R., Sørensen, E. and Voigt, H. O. (1988) Protein Eng. **2**, 157–166
28 Drejer, K., Kruse, V., Larsen, U. D., Hougaard, P., Bjørn, S. and Gammeltoft, S. (1991) Diabetes **40**, 1488–1495
29 Schäffer, L., Larsen, U. D., Linde, S., Hejnaes, K. R. and Skriver, L. (1993) Biochim. Biophys. Acta **1203**, 205–209
30 Graham, F. L. and Van der Eb, A. J. (1973) Virology **52**, 456–467
31 Scahill, S. J., Devos, R., Van der Heyden, J. and Fiers, W. (1983) Proc. Natl. Acad. Sci. U.S.A. **80**, 4654–4658
32 Andersen, A. S., Kjeldsen, T., Wiberg, F. C., Christensen, P. M., Rasmussen, J. S., Norris, K., Møller, K. B. and Møller, N. P. H. (1990) Biochemistry **29**, 7363–7366
33 Whitesell, R. R. and Gliemann, J. (1979) J. Biol. Chem. **254**, 5276–5283
34 De Meyts, P., Roth, J., Neville, D. M. J., Gavin, J. R. and Lesniak, M. A. (1973) Biochem. Biophys. Res. Commun. **55**, 154–161
35 De Meyts, P. (1994) Diabetologia **37** (Suppl. 2), S135–S148
36 McPherson, G. A. (1985) J. Pharmacol. Methods **14**, 213–228
37 Klein, H. H., Kowalewski, B., Drenckhan, M., Neugebauer, S. and Kotzke, G. (1993) Diabetes **42**, 883–890

38 Karnieli, E., Zarnowski, M. J., Hissin, P. J., Simpson, I. A., Salans, L. B. and Cushman, S. W. (1981) J. Biol. Chem. **256**, 4772–4777
39 Schäffer, L. (1994) Eur. J. Biochem. **221**, 1127–1132
40 Sasaoka, T., Draznin, B., Leitner, J. W. and Olefsky, J. M. (1994) J. Biol. Chem. **269**, 10734–10738
41 Sasaoka, T., Rose, D. W., Jhun, B. H., Saltiel, A. R. and Olefsky, J. M. (1994) J. Biol. Chem. **269**, 13689–13694
42 Zapf, A., Hsu, D. and Olefsky, J. M. (1994) Endocrinology (Baltimore) **134**, 2445–2452
43 Diguglielmo, G. M., Baass, P. C., Ou, W. J., Posner, B. I. and Bergeron, J. J. M. (1994) EMBO J. **13**, 4269–4277
44 Marshall, C. J. (1995) Cell **80**, 179–185
45 Avruch, J., Zhang, X. F. and Kyriakis, J. M. (1994) Trends Biochem. Sci. **19**, 279–283

Received 31 August 1995/26 October 1995; accepted 23 November 1995